Proc. Natl. Acad. Sci. USA
Vol. 87, pp. 1601–1605, February 1990
Biophysics

Dynamics of myoglobin: Comparison of simulation results with neutron scattering spectra

JEREMY SMITH*, KRZYSZTOF KUCZERA†, AND MARTIN KARPLUS

Chemistry Department, Harvard University, 12 Oxford Street, Cambridge, MA 01238

Contributed by Martin Karplus, November 3, 1989

ABSTRACT **Molecular dynamics simulations are used to calculate the incoherent neutron scattering spectra of myoglobin between 80 K and 325 K and compared with experimental data. There is good agreement over the entire temperature range for the elastic, quasi-elastic, and inelastic components of the scattering. This provides support for the accuracy of the simulations of the internal motions that make the dominant contributions to the atomic displacements on a time scale of 0.3–100 ps (100–0.3 cm^{-1}). Analysis of the simulations shows that at low temperatures a harmonic description of the molecule is appropriate and that the molecule is trapped in localized regions of conformational space. At higher temperatures the scattering arises from a combination of vibrations within wells (substates) and transitions between them; the latter contribute to the quasi-elastic scattering.**

Experimental and theoretical studies of the internal dynamics of proteins can provide insight into the atomic interactions determining their structure and function (1). In heme proteins such as myoglobin, the internal motions have been shown to have an essential role in ligand binding (1–9). Two extreme models for the internal motions have been considered. In one the fluctuations are assumed to occur within a single multidimensional well that is harmonic or quasiharmonic (10). The other model assumes that there exist multiple minima or substates on the protein potential surface (2, 5, 11, 12); the internal motions correspond to a superposition of oscillations within the wells and transitions among them (11). Photolysis rebinding studies (2, 5, 12) and simulations (11) of myoglobin provide strong evidence for the substate model, which may be generally applicable to globular proteins (12). The simulations have shown that structures associated with different substates are similar but differ in detail; for myoglobin the differences can be described in terms of rigid body displacements of the helices with rearrangements of the connecting loops and reorientation of the side chains involved in helix contacts. At low temperatures individual protein molecules are trapped in local regions of conformational space and static disorder, corresponding to an inhomogeneous macroscopic system, results; at higher temperatures transitions between the substates, which involve the crossing of energy barriers, are possible. Such behavior is analogous to that found in other complex systems (13).

Although much has been learned about protein motions from simulations, detailed experimental tests have been limited by the accessible time scales. Comparisons with x-ray, NMR, and fluorescence depolarization data have provided evidence that supports the simulation results (1), although it was suggested on the basis of the Mössbauer spectrum of myoglobin that the time scale of the simulated atomic fluctuations is two orders of magnitude too short (14); a reinterpretation of the results shows there is no inconsistency between the Mössbauer and simulation dynamics (15).

The publication costs of this article were defrayed in part by page charge payment. This article must therefore be hereby marked "*advertisement*" in accordance with 18 U.S.C. §1734 solely to indicate this fact.

Incoherent neutron scattering, which arises from self correlations in the atomic motions, is of particular interest because the experimental time scale of about 0.3–100 ps (100–0.3 cm^{-1}) falls in the range most commonly probed by molecular dynamics simulations (16–18). The incoherent neutron scattering from proteins is dominated by contributions from (nonexchangeable) hydrogen atoms. As about half of the atoms in a protein are hydrogens and as they are distributed throughout the molecule (mainly in the side chains), such scattering experiments provide a good test of the simulations.

In this paper we present calculations of the neutron scattering of myoglobin calculated from molecular dynamics simulations over the temperature range 80–325 K. The magnitude and temperature dependence of the theoretical elastic, quasi-elastic, and inelastic neutron scattering are in general agreement with recently obtained experimental results for myoglobin powder hydrated to 0.38 g of ^2H_2O per g protein (19). The comparison is of general interest because the protein powder is fully hydrated and is expected to have a structure corresponding to that in solution and to be biologically active (20–22). Use of a hydrated powder in the neutron scattering experiments yields better data than a solution study due to the higher concentration of the protein and the lower background from ^2H_2O. The comparison provides direct evidence for the accuracy of the molecular dynamics simulations over the entire temperature range and for a normal mode description at low temperatures. Further, analysis of the simulation permits us to interpret the dynamical phenomenona that underlie the experimental observations in terms of the quasi-harmonic and substate models.

Theoretical Method

The molecular dynamics simulations of myoglobin were performed using the polar hydrogen model and program CHARMM (23). A fuller description of the simulations will be published elsewhere (24). They consist of a 120-ps trajectory at 325 K and 50-ps trajectories at 240 K, 160 K, and 80 K; shorter simulations are sufficient at low temperatures because the displacements converge in the time period employed. The protein was studied in isolation and no attempt was made to mimic explicitly the interactions in the powder system used in the experiments. The utility of comparing vacuum simulations with experiments on powder and crystal systems has been demonstrated previously (1, 25, 26). The neutron spectral profiles and absolute intensities from dry powders have been shown to be similar to those from vacuum harmonic dynamic calculations with the CHARMM energy function (25, 26).

To compare with the neutron scattering, the molecular dynamics trajectories were used to compute the incoherent

*Present address: Laboratoire de Modelisation Moleculaire, Departement de Biologie, Institut de Recherche Fondamentale, Commissariat a l'Energie Atomique, Centre d'Etudes Nucléaires Saclay, 91191 Gif-sur-Yvette Cedex, France.
†Permanent address: Institute of Physics, Polish Academy of Sciences, Al.Lotnikow 32/46, 02-668 Warsaw, Poland.

dynamic structure factor, $S(\mathbf{q}, \omega)$, where $\hbar\omega$ is the energy transferred between the sample and the incident neutron, and $\hbar q$ is the momentum transfer. The function $S(\mathbf{q}, \omega)$ is the time Fourier transform of the intermediate scattering function, $F(\mathbf{q}, t)$, given by (17)

$$F(\mathbf{q}, t) = \sum_L b^2 \langle e^{-i\mathbf{q}\cdot\mathbf{r}_L(0)} e^{i\mathbf{q}\cdot\mathbf{r}_L(t)} \rangle_T, \quad [1]$$

where the sum is over the nonexchangeable hydrogen atoms in the protein, $\mathbf{r}_L(t)$ is the position vector of the Lth hydrogen atom at time t, b is the incoherent scattering length of hydrogen, and $\langle \ldots \rangle_T$ represents an ensemble average that is replaced by a time average over the molecular dynamics trajectory. The function $F(\mathbf{q}, t)$ was calculated directly from the protein trajectories and numerically Fourier transformed to obtain $S(\mathbf{q}, \omega)$. For comparison with the experimental results, $S(\mathbf{q}, \omega)$ was averaged over three orientations of the scattering wave vector (parallel to the molecular x, y, and z axes). Details of the method are given elsewhere (26, 27).

Results

In what follows we compare the calculated and experimental results for the elastic, quasi-elastic, and inelastic neutron scattering and use the simulation to provide an understanding of the motions that contribute to the various components of the scattering.

The elastic incoherent scattering, $S(\mathbf{q}, \omega = 0)$, can be related to the mean-squared displacement, $\langle \Delta x_L^2 \rangle$ for the nonexchangeable hydrogen atoms. In the Gaussian approximation, we have

$$S(q, \omega = 0) \approx \sum_L b^2 e^{-q^2 \langle \Delta x_L^2 \rangle}. \quad [2]$$

Eq. 2 is exact in the limit as $q \to 0$ and we can write

$$\langle \Delta x^2 \rangle = \sum_L \frac{\langle \Delta x_L^2 \rangle}{N} = -\frac{1}{Nb^2} \frac{\delta S(q, 0)}{\delta q^2}. \quad [3]$$

The measured $\langle \Delta x^2 \rangle$ is directly comparable with the corresponding quantity obtained from the simulations. It has an advantage over the more widely studied x-ray temperature factors in that there is no direct static disorder contribution (28). It should be noted, however, that the low-temperature $\langle \Delta x^2 \rangle$ measured by inelastic neutron scattering is affected by inhomogeneity—i.e., for a macroscopic system composed of molecules in different substates the experimental value is an average of the molecular $\langle \Delta x^2 \rangle$ values. Comparisons of two 80 K simulations with different average structures indicate that this effect is small (24). Fig. 1 shows the temperature dependence of the experimental $\langle \Delta x^2 \rangle$ values and those calculated from the simulations. Good agreement between experiment and theory is evident over the entire temperature range. Both the measured and calculated values indicate that there is a transition above which $\langle \Delta x^2 \rangle$ increases more rapidly with temperature. The experimental results show a (glass) transition between 180 K and 200 K. The theoretical transition is less well defined because of a lack of points in the intermediate temperature range; additional simulations are necessary to better characterize the form of the theoretical curve. The $\langle \Delta x^2 \rangle_{Fe}$ of the iron calculated from the simulations has a temperature dependence similar to that of the nonpolar hydrogens, but the magnitude is about a factor of 3 smaller (24). This is in agreement with estimates from Mössbauer spectroscopy (29).

More information concerning the atomic motion can be obtained from the q dependence of the elastic scattering. Fig. 2 shows ln $S(q, 0)$ as a function of q^2 obtained from the calculated atomic fluctuations. The solid lines were determined

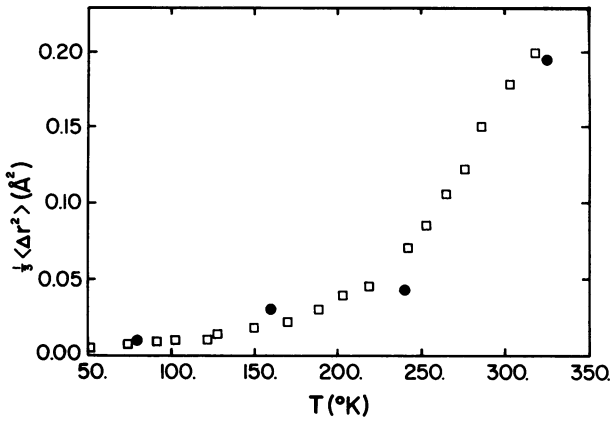

FIG. 1. Temperature dependence of the isotropically averaged mean squared displacements of myoglobin, $\frac{1}{3}\langle \Delta r^2 \rangle$, averaged over the exchangeable hydrogens. □, From the neutron experiment; ●, from molecular dynamics simulations.

using Eq. 2 and the dashed lines show the $q \to 0$ limiting behavior of ln $S(q, 0)$. Good agreement is seen between the form of the theoretical and experimental curves (see figure 1 of ref. 19). For the low-temperature simulation (80 K) the scattering is Gaussian (linear in q^2), but at higher temperatures a non-Gaussian component is evident. The non-Gaussian component appears in Fig. 2, although the scattering from each atom is modeled as a Gaussian. This is due to the fact that the hydrogen atoms in the protein are nonequivalent and have a distribution of $\langle \Delta x_L^2 \rangle$ values, as shown previously in simulations and x-ray analyses (1, 30). This nonequivalence, which increases with temperature in the simulations (24), becomes apparent when $q^2 \langle \Delta x_L^2 \rangle$ terms are too large for the expansion of the exponential to $0(q^2)$, as in Eq. 2, to be valid. Thus, in contrast to the conclusion based on experiment alone (19), it is not necessary to invoke non-Gaussian atomic dynamics to explain the non-Gaussian high-temperature behavior of the measured elastic scattering. The high-temperature experimental results were interpreted as being Gaussian in q at high q and non-Gaussian at low q (19). If the atomic motions are Gaussian with a distribution of $\langle \Delta x^2 \rangle$ values, one expects the reverse to be the case—i.e., non-Gaussian elastic scattering would become significant at higher q values. This is what gives the nonlinear form of the theoretical curves in Fig. 2, which correspond to the experimental results. High-temperature anharmonic contributions to the dynamics introduce an additional non-Gaussian component in the elastic scattering (19, 31). The kurtosis from 300 K simulations of myoglobin and

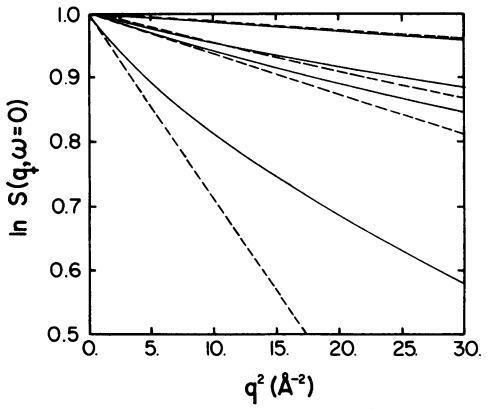

FIG. 2. Temperature dependence of the elastic intensity calculated from the simulations, using Eq. 2 (solid lines). The four solid lines and associated dashed lines (limiting slopes as $q \to 0$) are from the simulations at 80, 160, 240, and 325 K in order from top to bottom.

lysozyme indicate that for proteins at room temperature this contribution may be significant (32).

The quasi-elastic and inelastic neutron scattering spectra arise from the transfer of energy between the neutrons and the hydrogen atoms of the protein. This is described by structure factor, $S(\mathbf{q}, \omega)$, for $\omega \neq 0$. Fig. 3 shows $S(q, \omega)$ as a function of ω obtained from the Fourier transform of Eq. 1 calculated from the simulation; the elastic scattering has not been included and the low-energy cutoffs in the calculated curves are determined by the length of the simulations. The curves in Fig. 3, shown as a log–log plot, can be compared with the experimental data in figure 3 of ref. 19. Quasi-elastic scattering is normally associated with long time scale stochastic dynamics and typically consists of one or more Lorentzians centered at zero frequency (17, 31). In small molecules inelastic scattering consists of vibrational peaks well separated from the quasi-elastic frequency region. For proteins the quasi-elastic and inelastic scattering can arise from processes with similar time scales, so that there is some overlap of the spectral profiles. From Fig. 3, the smooth curve that comprises the 325 K scattering of ω less than 0.7 meV (6 cm^{-1}) is quasi-elastic and the inelastic scattering causes the peaks visible at higher frequencies. The form and temperature dependence of the calculated spectra are in good agreement with those obtained experimentally (19). At low temperatures the scattering profile is mainly inelastic, whereas at temperatures above 160 K, the quasi-elastic component is more important. The inelastic peaks are due to vibrations in the protein. Similar peaks in the same frequency range are seen in the scattering calculated from normal mode analyses of myoglobin and other proteins (refs. 25–27, 33, and 34; B. Tidor and M.K., unpublished); the modes in the frequency range under consideration are generally delocalized over the molecule.

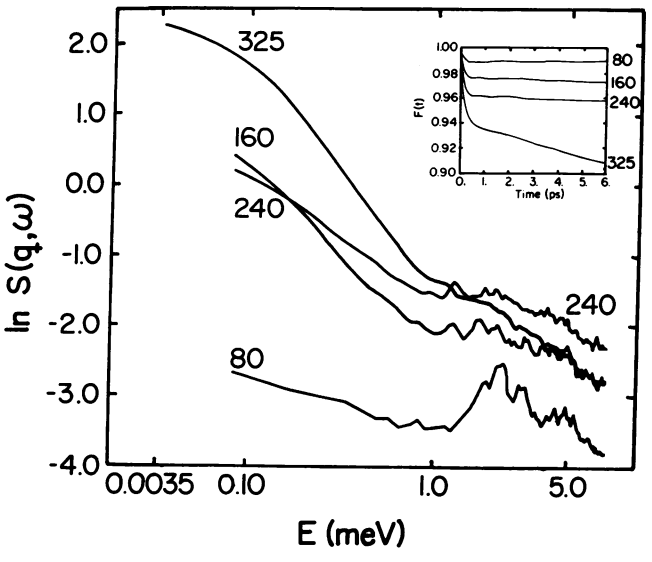

FIG. 3. A log–log plot of quasi-elastic and inelastic neutron spectra obtained from molecular dynamics simulations of myoglobin as a function of temperature. The spectra were derived by numerical Fourier transformation of $F(\mathbf{q}, t)$ (Eq. 1) at a constant scattering wave vector of $\mathbf{q} = 1$ $Å^{-1}$ and an energy resolution of 0.5 cm^{-1}. The experimental spectra in figure 3 of ref. 19, which are to be compared with the present results, comprise data at varying q values; for the low-frequency range plotted here the form of the spectrum is only slightly dependent on the value of $\mathbf{q}$. In addition, the experimental spectrum in ref. 19 was modified by subtracting an approximation to the vibrational scattering, assuming the frequencies and forms of the modes are invariant with temperature (see text). No such subtraction was made in the present figure. (*Inset*) The correlation function, $F(\mathbf{q}, t)$, from the simulations.

The experimental scattering was analyzed in terms of a slow quasielastic "α" process and a "β" region of scattering at higher energy transfers (19). The α process corresponds to the calculated smooth quasielastic curve. Analysis of this curve shows that over the frequency range of the smooth α curve (between 0.04 and 0.9 meV or 0.3 and 7.0 cm^{-1}) can be approximated by a Lorentzian,

$$S(q, \omega) = A/(1 + \tau^2\omega^2), \quad [4]$$

where at 325 K, $A = 9 \pm 1$ and $\tau = 5.5 \pm 0.7$ ps; these results are in agreement with the experimental estimates.

Shorter time scale (β) scattering appears at frequencies above 0.7 meV (6 cm^{-1}) in both the calculated and experimental spectra as a deviation from the extrapolated α line. In the experimental analysis (19) the 80 K experimental vibrational contribution was scaled to higher temperatures and subtracted from the observed scattering. The remaining scattering in the β region was identified as an additional quasi-elastic process. Fig. 3 shows that the form of the vibrational contribution changes with temperature in a manner consistent with increased frictional damping of modes at higher temperatures—i.e., at higher temperatures the vibrational peaks are smoothed. Scaling of the calculated 80 K results to 325 K, assuming harmonic dynamics, yields scattering slightly larger in magnitude than that obtained from the 325 K simulation and shows that the modes shift to lower frequencies with increasing temperature. This is in accord with the heme group results (see below and Fig. 5). A quantitative determination of the vibrational contribution to the β region scattering by simple subtraction of the scaled 80 K scattering, thus, appears difficult. In any case, the simulations do not provide clear evidence for an additional, β, quasi-elastic process, although it is possible that the calculated magnitudes are somewhat in error.

Fig. 3 *Inset* shows the time correlation functions obtained from Eq. 1. In all cases there is an initial fast decay. The time constant for this decay is 0.3 ps ± 0.1 ps for the 80 K, 160 K, and 240 K simulations. The fast relaxation process is associated with the dephasing of the vibrational modes. Similar rapid decay behavior is seen generally in molecular dynamics simulations of proteins (15) and in $F(\mathbf{q}, t)$ calculated from a protein normal mode analysis (27). For the three low temperatures a plateau in the time correlation function is reached, the level of which is determined by the mean squared displacements (17). At 325 K the time constant of the initial decay is 0.5 ps ± 0.1 ps, which is somewhat longer than the lower temperature value. This is in agreement with the measured results (inset of figure 3, ref. 19). The change in time constant is consistent with the modifications to the vibrational dynamics seen in Fig. 3 and/or the presence of additional anharmonic processes. Also visible in the 325 K correlation function is a slower relaxation that is associated with the α quasi-elastic scattering and was also seen in the experiment. A slow decay was seen experimentally at 240 K but is not found in the calculations. This fact, taken together with the relatively intense 240 K vibrational scattering in Fig. 3, suggests that certain aspects of the 240 K calculated dynamics are more similar to 160 K and 80 K than to 325 K. Thus, the transition range in the dynamics may be at a somewhat higher temperature in the vacuum simulations than in the experiment.

In general, the experimental spectra, particularly those at higher temperatures, are smoother than the calculated results. Possible contributing factors are instrumental resolution broadening (33) and solvent frictional damping (27). An additional effect arises as inhomogeneous broadening associated with the averaging over different substates, which is expected to be important at the lower temperatures. Such averaging can be explored by comparing spectra from the two

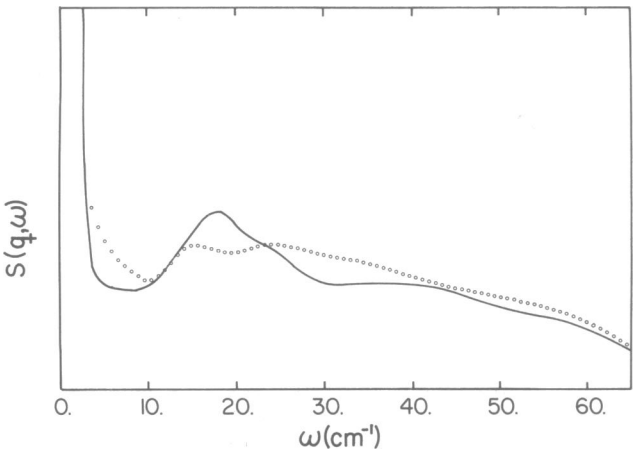

FIG. 4. The function $S(\mathbf{q}, \omega)$ calculated at $\mathbf{q} = 1$ Å^{-1} from two molecular dynamics simulations of myoglobin at 80 K. The scattering curves have been convoluted with the experimental instrumental resolution function.

different 80 K myoglobin molecular dynamics trajectories, which sample different regions of conformational space (24). The results are shown in Fig. 4, in which the spectra are calculated at the instrumental resolution of the experiments. In each of these two regions the dynamics is vibrational. As the molecule has a different average geometry in the two trajectories, the distribution of normal mode frequencies changes. This is manifested in the scattering profiles shown in Fig. 4. In an experimental sample, many such profiles would be averaged and a smoothed spectrum would result.

To provide more detailed information on the origin of the observed spectrum, we focus on a specific region of the protein. In Fig. 5 the scattering profiles calculated from the molecular dynamics simulations at 80 K and 325 K are shown for the heme group. This particular region is chosen for its functional interest and because the difference spectrum of a fully deuterated globin and one with a protonated heme group should be accessible experimentally. The 80 K spectrum shows clear peaks arising from low-frequency vibrational modes with no appreciable quasi-elastic scattering. At 325 K, corresponding vibrational peaks are still present, but they are superposed on a quasi-elastic background. Also, certain of the peaks are shifted to somewhat lower frequencies. In the calculated spectra from the entire protein at 80 K and 325 K (Fig. 3), there are certain similarities to the heme group results. For example, the three most intense peaks at 80 K (between 10 and 20 cm^{-1}) are also present at 325 K and they are shifted to lower frequencies by about 3 cm^{-1}. Since the vibrational spectrum from the heme group is simpler than that of the whole molecule (fewer modes contribute significantly to the scattering) an experimental study to test this analysis would clearly be of great interest. Calculations for atoms in other parts of the protein (e.g., specific side chains) are in accord with these results.

Concluding Discussion

The results described here have shown that molecular dynamics simulations of myoglobin over a wide range of temperatures yield incoherent neutron scattering spectra in general agreement with experiment. This is true in spite of the fact that vacuum simulations are being compared with experiments on hydrated powder samples. Since the calculated results depend on the model [e.g., dielectric function, cut-off for long-range interactions (35)], it is possible that environmental effects are included implicitly in the simulation procedure (24). Given the observed agreement one can use the

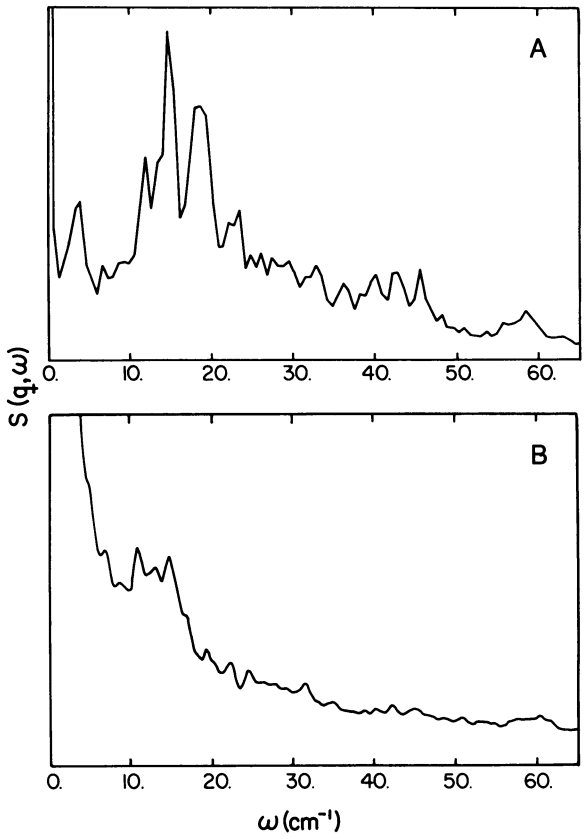

FIG. 5. The function $S(\mathbf{q}, \omega)$ calculated at $\mathbf{q} = 1$ Å^{-1} at 0.5 cm^{-1} resolution for the heme group in myoglobin. (*A*) The 80 K spectrum. (*B*) The 325 K spectrum.

simulation to determine the types of motions that contribute to the spectrum as a function of temperature. Of particular importance are the side chain motions [temperature-dependent oscillations and transitions of the dihedral angles (11, 19, 24)], since the only main chain contributions to the scattering come from the C^{α} hydrogens.

At low temperature (below 100 K), the atomic motions in proteins can be described in terms of harmonic vibrations. Each molecule is trapped in a region of conformational space for times (>100 ps) long compared to the neutron time scale. The average mean square fluctuation in such a well at 80 K is equal to about 0.025 Å^2, and the distribution of fluctuation magnitudes is very narrow (the average deviation is ±0.014 Å^2 at 80 K). The time decay of the intermediate scattering function is dominated by vibrational dephasing. There is some inhomogeneous broadening of the neutron spectra due to the fact that a macroscopic sample is made up of protein molecules trapped in different substates. As the temperature is raised, there is a slight softening of a few modes (shift to lower frequencies) and the time for transitions between wells is reduced so that a larger region of conformational space is explored by the molecule on the time scale of the neutron scattering experiment. Thus, $\langle \Delta x^2 \rangle$ increases more rapidly with temperature than expected from the harmonic approximation and the distribution of fluctuation magnitudes broadens significantly. The softening of vibrational modes is consistent with a quasi-harmonic model for the dynamics (10) in which the atomic motions at any given temperature are essentially harmonic but the force constants decrease with increasing temperature. Within the quasi-harmonic approximation, the incoherent elastic scattering from individual atoms is Gaussian in q and the calculated total elastic scattering is in agreement with experiment.

The increased importance of quasi-elastic scattering at higher temperatures suggests that additional anharmonicity is present. The simulations show that anharmonic contributions arise from transitions among substates that are on the time scale of the quasi-elastic scattering (11, 24). At room temperature the transition times range from 0.1 ps to 100 ps depending on the distances between wells and the barriers between them (11). As mentioned in the Introduction, the calculated transitions are complex in nature and involve significant backbone as well as side chain displacements; torsional angle transitions play only a minor role. Another contribution to quasi-elastic scattering within the quasi-harmonic model would arise from overdamped harmonic modes (27). The elastic scattering from individual atoms described by such Langevin oscillators would be Gaussian in q. Although the simulation results are consistent with increased damping of the vibrational modes at higher temperatures, most of the low-frequency protein modes remain underdamped at 325 K.

The inclusion of explicit environmental effects (e.g., aqueous solvation, powder neighbor interactions) in the simulation would introduce additional damping and modify the effective potential experienced by the individual atoms. It is of interest that the effects on the neutron spectra of hydrating a protein are rather similar to increasing the temperature. Measured room temperature spectra from proteins at low hydration can be approximately reproduced by harmonic models of the internal dynamics (25). At higher hydrations there is a quasi-elastic component to the scattering (36).

The present comparison of vacuum simulation and hydrated powder experiments is suggestive concerning the effect of the environment on the atomic potentials of mean force. It appears that the form of the individual wells in which the atoms vibrate at low temperatures is not sensitive to solvent for many of the atoms in the protein interior. However, the nature of the barriers between the wells may be more perturbed by the environment. It is the latter that determine the transition in the temperature dependence of $\langle \Delta x^2 \rangle$ and the quasi-elastic contribution to the scattering. The variation of the myoglobin transition temperature with solvent is in accord with this conclusion (37).

The possible role of selective protonation of the deuterated protein as a technique for obtaining more detailed data has been illustrated by the heme group results. For such a study a neutron source of higher flux would be desirable. It is encouraging that a powerful neutron source is planned for the near future (38).

As has been pointed out recently (39), more work is required before theory and experiment are united in such a way that a full understanding of the internal motions of proteins and their functional roles can be achieved. The present results show one way in which insights into protein dynamics can be provided by the use of simulations to aid in the interpretation of experimental data. Of equal importance, the agreement between theoretical and experimental incoherent neutron scattering results provides a needed test of both the overall amplitude and time scales of the fluctuations calculated by molecular dynamics simulations of proteins.

We thank Stephen Cusack and Wolfgang Doster for stimulating discussions and John Straub and Bruce Tidor for helpful comments.

1. Brooks, C. L., III, Karplus, M. & Pettitt, B. M. (1988) *Proteins: A Theoretical Perspective of Dynamics, Structure, and Thermodynamics*, Advances in Chemistry and Physics (Wiley, New York), Vol. 71.
2. Austin, R. H., Beeson, K. W., Eisenstein, L., Frauenfelder, H. & Gunsalus, I. C. (1975) *Biochemistry* **14,** 5355–5373.
3. Frauenfelder, H., Petsko, G. A. & Tsernoglou, D. (1979) *Nature (London)* **280,** 558–563.
4. Debrunner, P. G. & Frauenfelder, H. (1982) *Annu. Rev. Phys. Chem.* **33,** 283–299.
5. Ansari, A., Dilorio, E. E., Dlott, D. D., Frauenfelder, H., Iben, I. E. T., Langer, P., Roder, H., Sauke, T. B. & Shyamsunder, E. (1986) *Biochemistry* **25,** 3139–3146.
6. Doster, W., Beece, D., Bowne, S. F., Dilorio, E. E., Eisenstein, L., Frauenfelder, H., Reinisch, L., Shyamsunder, E., Winterhalter K. H. & Yue, K. T. (1982) *Biochemistry* **21,** 4831–4839.
7. Parak, R., Knapp, H. W. & Kucheida, D. (1982) *J. Mol. Biol.* **161,** 177–194.
8. Keller, H. & Debrunner, P. (1980) *Phys. Rev. Lett.* **45,** 68–71.
9. Case, D. A. & Karplus, M. (1979) *J. Mol. Biol.* **132,** 343–368.
10. Levy, R., Karplus, M., Kushick, J. N. & Perahia, D. (1984) *Macromolecules* **17,** 1370–1374.
11. Elber, R. & Karplus, M. (1987) *Science* **325,** 318–321.
12. Frauenfelder, H., Parak, F. & Young, R. D. (1988) *Annu. Rev. Biophys. Biophys. Chem.* **17,** 451–479.
13. Yu, C. C. & Leggett, A. J. (1988) *Comments Condensed Mater. Phys.* **14,** 231–251.
14. Parak, F. & Knapp, E. W. (1984) *Proc. Natl. Acad. Sci. USA* **81,** 7088–7092.
15. Nadler, W., Bruenger, A. T., Schulten, K. & Karplus, M. (1987) *Proc. Natl. Acad. Sci. USA* **84,** 7933–7937.
16. Middendorf, H. D. (1984) *Annu. Rev. Biophys. Bioeng.* **13,** 425–451.
17. Lovesey, S. (1984) *Theory of Thermal Neutron Scattering from Condensed Matter* (Clarendon, Oxford).
18. Cusack, S. (1986) *Comments Mol. Cell. Biophys.* **3,** 243–271.
19. Doster, W., Cusack, S. & Petry, W. (1989) *Nature (London)* **337,** 754–755.
20. Rupley, J. A., Gratton, E. & Careri, E. (1983) *Trends Biochem. Sci.* **8,** 18–22.
21. Finney, J. L. & Poole, P. L. (1984) *Comments Mol. Cell. Biophys.* **2,** 129–151.
22. Poole, P. L. & Finney, J. L. (1983) *Int. J. Biol. Macromol.* **5,** 308–310.
23. Brooks, B., Bruccoleri, R., Olafson, B., States, D., Swaminathan, S. & Karplus, M. (1983) *J. Comp. Chem.* **4,** 187–217.
24. Kuczera, K., Kuriyan, J. & Karplus, M., *J. Mol. Biol.*, in press.
25. Cusack, S., Smith, J., Tidor, B., Finney, J. L. & Karplus, M. (1988) *J. Mol. Biol.* **202,** 903–908.
26. Smith, J., Cusack, S., Tidor, B., Kuczera, K., Doster, W. & Karplus, M. (1989) *Physica B (Amsterdam)* **156–157,** 437–443.
27. Smith, J., Cusack, S., Tidor, B. & Karplus, M., *J. Chem. Phys.*, in press.
28. Hartmann, H., Parak, F., Steigemann, W., Petsko, G. A., Ringe-Ponzi, D. & Frauenfelder, H. (1982) *Proc. Natl. Acad. Sci. USA* **79,** 4967–4971.
29. Nienhaus, G. U., Heinzl, J., Huenges, E. & Parak, F. (1989) *Nature (London)* **338,** 665–666.
30. Post, C. B., Brooks, B. R., Dobson, C. M., Artymiuk, P., Cheetham, J., Phillips, D. C. & Karplus, M. (1986) *J. Mol. Biol.* **190,** 455–479.
31. Bee, M. (1988) *Quasielastic Neutron Scattering: Principles and Applications in Solid State Chemistry, Biology and Materials Science* (Hilger, Bristol, U.K.).
32. Kuriyan, J., Petsko, G. A., Levy, R. M. & Karplus, M. (1986) *J. Mol. Biol.* **190,** 227–254.
33. Smith, J., Cusack, S., Pezzeca, U., Brooks, B. & Karplus, M. (1986) *J. Chem. Phys.* **85,** 3636–3654.
34. Cusack, S., Smith, J., Finney, J., Karplus, M. & Trewhella, J. (1986) *Physica B (Amsterdam)* **136,** 256–259.
35. Longcharich, R. J. & Brooks, B. R. (1989) *Proteins Struct. Funct. Genet.* **6,** 32–45.
36. Smith, J., Cusack, S., Poole, P. L. & Finney, J. L. (1987) *J. Biomol. Struct. Dyn.* **4,** 583–588.
37. Iben, I. E. T., Braunstein, D., Doster, W., Frauenfelder, H., Hong, H., Johnson, M. K., Luck, J. B., Ormos, P., Schulte, A., Steinbach, P. J., Xie, A. H. & Young, R. D. (1989) *Phys. Rev. Lett.* **62,** 1916–1919.
38. Moon, R. M. & West, C. D. (1989) *Physica B* **156–157,** 522–524.
39. Frauenfelder, H. (1989) *Nature (London)* **338,** 623–624.